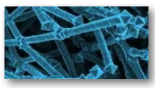
Materiales

Revista Mexicana de Ingeniería Química

Vol. 13, No. 3 (2014) 897-906

PREPARATION OF CELLULOSE NANOPARTICLES FROM AGAVE WASTE AND ITS MORPHOLOGICAL AND STRUCTURAL CHARACTERIZATION

PREPARACIÓN DE NANOPARTÍCULAS DE CELULOSA A PARTIR DE DESECHOS DE AGAVE Y SU CARACTERIZACIÓN MORFOLÓGICA Y ESTRUCTURAL

C.E. Ponce-Reyes[1], J.J. Chanona-Pérez[1*], V. Garibay-Febles[2], E. Palacios-González[2], J. Karamath[2], E. Terrés-Rojas[2], G. Calderón-Domínguez[1]

[1]*Departamento de Ingeniería Bioquímica, Prolongación de Carpio y Plan de Ayala s/n, Col. Santo Tomas C.P. 11340 Miguel Hidalgo. Escuela Nacional de Ciencias Biológicas, Instituto Politécnico Nacional. México, D.F.*

[2] *Laboratorio de Microscopia de Ultra Alta Resolución, Eje Central Lázaro Cárdenas Norte 152 Col. San Bartolo Atepehuacan C.P 07730 Gustavo A. Madero. Instituto Mexicano del Petróleo. México, D.F.*

Received May 9, 2014; Accepted June 20, 2014

Abstract

Agave is a natural waste from many different industries in Mexico, so alternative uses for these fibrous waste materials are desirable. Cellulose nanoparticles were obtained from dried agave leaves by acid hydrolysis. The characterization of the nanoparticles was made using scanning electron microscopy (SEM), Fast Fourier transformation infrared (FTIR) solid state nuclear magnetic resonance (ssNMR), X-ray diffraction (XRD) and high resolution transmission electron microscopy (HR-TEM). The nanoparticles had an average size of 97 ± 30 nm within a range of 31-198 nm, with a quasi-spherical and polyhedral morphology associated to a shape factor of 0.78 ± 0.06. The FTIR results revealed that the cellulose nanoparticles showed the characteristic cellulose peaks. Meanwhile, ssNMR showed the main peaks of the cellulose there was a difference in the peaks presence and absence when comparing to the cellulose pattern, which was associated to a lower crystallinity of the agave nanoparticles. In addition, the nanoparticles had a triclinic crystalline structure and a crystallinity index of 39% confirmed by HR-TEM and XRD. This study is important for a facile obtention of green nanomaterials from agroindustrial waste.

Keywords: agave waste, cellulose nanoparticles, crystallinity, microscopy, spectroscopy.

Resumen

El agave es un deshecho natural de diferentes industrias de México, por lo tanto, los usos alternativos de estos deshechos fibrosos son deseables. Nanopartículas de celulosa fueron producidas desde hojas de agave deshidratadas por hidrolisis acida. La caracterización de estas nanopartículas se llevó a cabo mediante microscopia electrónica de barrido (SEM), espectroscopia infrarroja con transformada de Fourier (FTIR), difracción de rayos X (XRD), resonancia magnética nuclear de estado sólido (ssNMR) y microscopia electrónica de transmisión de alta resolución (HRTEM). Las nanopartículas tuvieron un tamaño promedio de 97 ± 30 nm en un intervalo entre 31-198 nm y con morfología cuasi-esférica y poliédrica asociado a un factor de forma de 0.78 ± 0.06. Los resultados de la FTIR revelaron que las nanopartículas poseen los picos característicos de la celulosa, mientras que el espectro de ssNMR confirmó su naturaleza celulósica. Sin embargo, hubo diferencia en la presencia de picos en comparación con el espectro de la celulosa patrón, que fue asociado a una menor cristalinidad de las nanopartículas de agave. Además, las nanopartículas tuvieron una estructura cristalina triclínica y un índice de cristalinidad del 39 %, lo cual fue establecido mediante HRTEM y XRD. Este estudio es importante para la fácil obtención de nanomateriales verdes desde residuos agroindustriales.

Palabras clave: desechos de agave, nanopartículas de celulosa, cristalinidad, microscopía, espectroscopía.

*Corresponding author. *E-mail*: jorge_ chanona@hotmail.com

1 Introduction

The word agave comes from the Greek *agavos* whose meaning is "admirable" or "noble". The gender agave is from America, especially Mexico, from where it has been taken to other countries (Gil *et al*., 2001). Agave consists of 155 species of which 116 (75% of the total) are only found in Mexico (Hubbe *et al*., 2008). Agave grows in the semi-dry cold highlands of Mexico, mainly in the Central Valley and in the Mexican states of Hidalgo, Puebla and Tlaxcala. In Mexico, agave has had a great economic and cultural importance to numerous indigenous people, who have taken advantage of it for centuries as food, drink, medicine, fuel, shelter, ornament, etc. Their leaves are very substantial, fibrous and fleshy; those from smaller species may weigh no more than 20 g, while those from the larger species ("pulquero") can weigh more than 30 kg each and their maturity period is between 6 and 8 years. The 62 % of the production of agave is used to produce tequila and mezcal; however they only use 40% of the agave; 60% of the product never reaches the market. Some agaves are used to produce alcoholic beverages and agave fibrous wastes also can be used as source for paper-making fibers and fertilizers (Narvaez-Zapata and Sanchez-Teyer, 2009).

Agave tissues include chemical components such as cellulose (40-80%), lignin (5-25%) and hemicelluloses (10%); this chemical composition results in hardness and stiffness (Macia, 2006; Hepworth, 2000). Cellulose is a glucose polymer present in plants, non-soluble in water and with an important structural function. It has a high molecular weight (3000 glucose units) and its chains have no ramifications. One important characteristic are the β (1-4) bonds between its glucose units. It has an arrangement in which the hydroxyls generate strong intermolecular bonds, acquiring crystalline properties (Hepworth, 2000). Currently, many patents describe the utilization of byproducts of Agave species used on alcoholic beverages production. For example, the leaves of *A. tequilana*, are commonly discarded after obtaining the core, but these can be used to produce a good quality fiber. This can be mixed with a thermosetting polymer resin to manufacture several products (Tang and Chow, 2006). However, no patents exist for the use of Agave as a cellulose nanoparticles source. On the other hand, in the last few decades, the interest in sustainability and green chemistry has been growing, which has led to an awareness in new compounds (Gradwell *et al*., 2004) and biomaterials (Ragauskas *et al*., 2006) derived from different cellulosic sources (Samir *et al*., 2005).

From these materials, various products have been developed such as cellulose whiskers with lengths of approximately 100 nm and diameters of 3-20 nm, prepared by acid hydrolysis of cellulose fibers (Zhang *et al*., 2007). Previous analyses made by Hepworth (2000), such as X-ray diffraction (XRD) and infrared absorption have demonstrated that the cellulose fibers consist of crystalline and amorphous regions. The crystalline regions of the chains are ordered in a microcrystalline form, which allows the formation of macroscopic micelles. Cellulose presents a high crystalline degree, but it is not 100% crystalline, the presence of hemicelluloses could cause disturbances in the crystallinity, which explains why cellulose is not soluble in aqueous solvent systems (Coronel, 1994). The crystalline system present in nature is cellulose I, however, when it is treated with an aqueous alkaline solution, cellulose II could be obtained (Colodette, 1989). Cellulose I possess a unitary cell denominated monoclinic while cellulose II possess a unitary cell denominated triclinic, meaning all of its angles are different from 90° and different among them. Their sides are different too. Cellulose II is thermodynamically more stable than cellulose I due to the hydrogen bonds (Blackwell *et al*., 1987).

Cellulosic nanoparticles, better known as nanocellulose, have generated scientific interest because of their availability, low cost, biodegradability, strength and other characteristics. Different descriptors are used in the literature to designate these crystalline rod-like nanoparticles. They are mainly referred as whiskers, nanowhiskers, cellulose nanocrystals, NCC (nanocrystalline cellulose), monocrystals, microcrystals or microcrystallites, despite their nanoscale dimensions (Siqueira *et al*., 2009). However, the dimensions of cellulosic nanoparticles depend on several factors, including the source of cellulose and the exact preparation conditions (Hubbe *et al*., 2008). Nowadays, organic nanoparticles are being synthesized due to its importance in many industries such as food, packaging, medicine, paintings, etc. (Cruz-Estrada *et al*., 2006; Kallioranta, 2012). In case of cellulose nanofibers, they are been used in electronics, medicines and many other industries as a reinforcement material. These nanoparticles are relevant because of their functionality, easy synthesis, properties, biodegradability and biocompatibility. However, spherical cellulose nanoparticles have not widely been used in the industry yet (Qing *et al*., 2012). Due to this, the aim of this work was to

hydrolyze the agave material to obtain cellulose nanoparticles, which could be used as reinforcement materials in the food, packaging and bio-plastic materials, electronics and pharmaceutical industries.

2 Materials and methods

2.1 Materials

Hydrochloric acid (12.1 N HCL), 36 N sulfuric acid (H_2SO_4) and dimethyl sulfoxide (DMSO) were purchased from Fermont (Monterrey, Mexico). Sodium hydroxide, pellets were supplied by Meyer (USA). Microcrystalline Cellulose (MCC) was purchased from Sigma/Aldrich (USA). Agave atrovirens parenchymatous tissue was obtained from the waste of the plants cultivated in a plantation established in the countryside of Mexico City. The plants were between six years of age, before the age of flowering (*quiote*).

2.2 Obtention of Agave fibers and preparation of nanoparticles

The tissue was dehydrated by convective drying using a tunnel dryer at 60 °C and an air flow of 3 m/s as reported by Gumeta *et al*., (2011). The dehydrated material was passed through a conventional mill (Picalica, Moulinex, France) to reduce particle size and then passed through a no. 8 sized mesh to sieve out particles of less than 2.36 μm. A 0.6 g sample of the agave particles was transferred to a 5.00 M NaOH solution (20 ml) and heated to 80°C for 3 hours with constant agitation. This alkaline treatment is done to remove the lignin from the fibers. After 3 hours, the sample was filtered and washed with deionized water until it attained a pH 7 (Bolio-Lopez *et al*., 2011). To the resulting cellulose, 20 ml of DMSO was added and then the sample warmed for 3 hours to 80°C. The sample was then filtered and washed several times with deionized water to remove the remaining lignin and hemicelluloses.

The fibers were transferred to an acid solution consisting of HCl, H_2SO_4 and deionized water (in a 1:3:6 ratio respectively), and then dispersed using an ultrasonic bath with internal heater (Fisher Scientific, FS-60D, USA) at 80°C for 3 hours. After this time period, the result is a milky colloidal suspension which had to be neutralized with a 2N NaOH solution and then placed in a centrifuge (Microspin12, Boeco, Germany) at 2000 RCF for 10 minutes. The residual fraction was dialyzed (Spectra/Por dialysis membrane WCO: 1000, Spectrum laboratories, USA) against deionized water. The resulting cellulose nanoparticles (CNP) were then characterized.

2.3 Spectroscopic characterization

FTIR was used to detect functional groups in the MCC and the CNP and confirm their cellulosic nature. For this reason Fourier transformation infrared (FTIR) spectra were obtained using a spectrometer LabRam HR800 (Horiba Jobin Yvon; Miyanohigashi, Kyoto, Japan) using IlliminatIR II with a spectral range of 400-4000 cm^{-1} according to reported by Baker *et al*., (2005).

Crystallinity index or percent crystallinity (X_{CR}) was measured from the obtained nanoparticles and the cotton microcrystalline cellulose (MCC) (Aldrich, USA) diffractograms and was used as a comparative reference due to its high crystallinity value. Diffractograms were obtained using XRD (D-8 Discover, USA) and the measurements were done using a Bragg-Bretano Geometry. The conditions to obtain the diffractograms were: scanning 2θ=0-70°, step time 300 s, step size 10 s, power 40 kV. X_{CR} was estimated using the Segal method (Thygesen *et al*. 2005). It was determined using the integral intensity (200) of peak (I_{200}, 2θ= 22.7°) and the minimum intensity between peak (200) and (110) (I_{AM} 2θ = 18°), where I_{200} represents the sum of crystalline and amorphous regions and I_{AM} represents only the amorphous region. The expression used was:

$$X_{CR} = \frac{I_{200} - I_{AM}}{I_{200}} \times 100 \qquad (1)$$

The result was expressed as percentage of crystallinity. Additionally, to compare the peaks width of CNP and MCC, the full width at half maximum (FWHM) for peak I_{200} (2θ= 22.7°) was estimated from fit of spectrum by means of a Lorentzian function and using SigmaPlot v 12.5 (Systat Software, Inc. USA).

The ^{13}C ssNMR was carried out in a spectrometer (ASCEND 400 MHz, Bruker, Massachusetts, USA) spin 9,000 Hz and a transient number of 10240; the spectra were obtained at 400 MHz with a similar 5 mm high-speed probe. The relaxation measurements were made with a static, horizontal-coil probe, also operating at 400 MHz. This technique was used to corroborate the composi tion and crystallinity of the CNP.

2.4 Microscopy characterization

Characterization of the samples was made by field emission scanning electron microscopy (FE-SEM) using Dualbeam Nova200 SEM (FEI, Holland). Each FE-SEM sample was sonicated and dried in a desiccator. A drop of the sample was placed on a FE-SEM sample holder which had been previously covered with conducting carbon tape. Particle size and shape factor were measured from SEM micrographs using ImageJ v 1.34s (National Institute of Health, Bethesda, MD, USA) and a total of 300 particles were measured. The particle size distribution and descriptive statistics were determined by using SigmaPlot v 12.5 (Systat Software, Inc. USA). High resolution transmission electron microscopy (HRTEM) was used to study the molecular structure of CNP, the observations were performed at 300kV using a high resolution transmission electron microscope (TITAN, FEI, Holland). HRTEM samples were prepared in suspension with deionized water and placed in a sonic bath for 5 minutes, then dispersed on Lacey Carbon Grids and vacuum dried for 24 hours. The crystalline structure of the CNP was elucidated from the HRTEM images and the diffraction patterns according to the reported by Askeland (1987) and using Digital Micrograph software v 10.1 (Gatan, USA).

3 Results and discussion

3.1 Morphology and size distribution

Figure 1a show SEM images, CNP can be observed as agglomerates with heterogeneous sizes. This could be possible due to the cellulose-hemicellulose complex formation. This agglomeration is associated with the presence of residual hemicellulose as mentioned by Nyström *et al*., (2010). On the other hand, the Figure 1b show images of the nanoparticles that were dispersed by ultrasonication, where it is possible to observe that particles of nanometric size can be generated by this facile preparation method. This process disperses the agglomerates thus particles of less than a 100 nm are observed. Figure 1c shows the histogram of the particle size distribution of the cellulose nanoparticles as characterized by SEM. The distribution showed to be normal. Fitting the data to the model returned R^2 = 0.9673. This value indicates that the distribution model applied adequately describes the size distribution of the nanoparticles. The average particle size obtained was 97 ± 30 nm within a range of 31-198 nm. Also, the circularity was measured obtaining a shape factor of 0.78 ± 0.06 within a range of 0.61-0.93, this could be linked to the quasi-spherical and polyhedral particles observed under SEM (Figure 1b). These results agree with the ones obtained by Zhang *et al*. (2007), who obtain spherical nanoparticles too. However, the average particle size reported was 80 nm with dispersion between 60-570 nm using commercial cellulose as the source to synthesize nanoparticles. This indicates that the method employed in the present study, produced quasi-spherical and polyhedral nanoparticles with a smaller mean particle size and dispersion compared to those reported in other works. According to Garcia *et al*. (2010), the large aggregates obtained from the ultrasonication process are due to particle coalescence as a result of the particle-particle interphase.

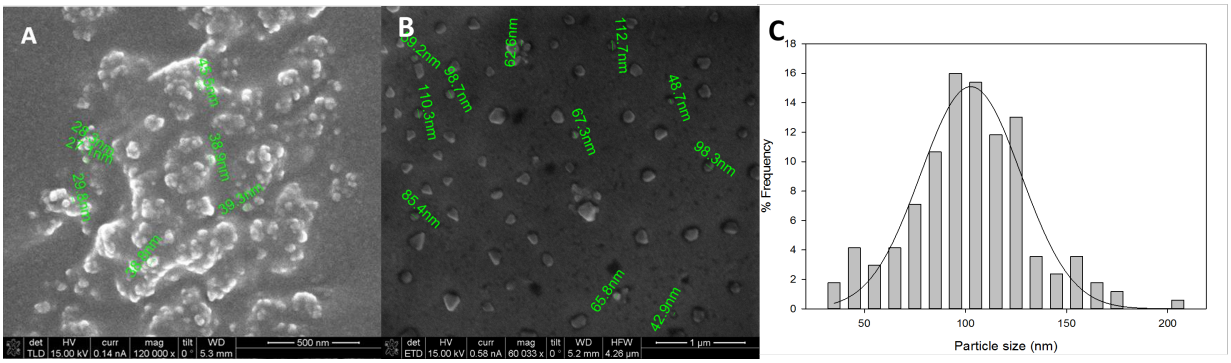

Fig. 1. A) SEM image of cellulose nanoparticles agglomerated B) SEM image of cellulose nanoparticles after ultrasonication C) Histogram of the particle size distribution.

There are no compounds in the system that can generate a repulsive force to keep the particles away from one another. There are studies reporting the production of nanoparticles from cotton fibers using alkaline-acid conditions (Elazzouzi-Hafraoui *et al*., 2008). These authors obtained elongated fibrils with an average length of 141 nm, average diameter of 20 nm and a distribution of particle sizes between 5 and 90 nm. Prior literature reports findings on nanowhiskers and/or nanofibrils (Ansari *et al*., 2010). These type of fibrils have also been obtained from the cell-wall of algae (Glaucocystis nostochinearum) resulting in similar diameters and lengths (Nishiyama *et al*., 2003). The shape of the nanomaterials (nanoparticles and nanofibrils) obtained in this work is different from both works mentioned above. Thus, the novelty here is the morphology of CNP, whilst nanometric in size is quasi-spherical and in some cases they adopted a polyhedral shape.

3.2 Spectroscopic characterization of the nanoparticles

FTIR spectra of MCC and CNP are shown in Figure 2. The spectra showed the characteristic absorption bands in 3412 cm^{-1} from the hydroxyls belonging to the cellulose. The carboxyl absorption band appears in 1646 cm^{-1}, while a peak is on the 1032 cm^{-1} band due the presence of glucans, meanwhile, there is a peak in the band 879 cm^{-1} belonging to the pyranoside ring (C-H ring), this data is similar to the one reported by Inpanya *et al*., (2012). MCC and CNP are different in the band intensity, this could be because the MCC is a pure material, while CNP could have impurities due to the obtention process and its particle size was smaller than the MCC.

The cellulose nanoparticles XRD is shown in Figure 3. It is clear that the material, obtained from agave, has a partial crystallinity. The crystallinity indexes for MCC and CNP were 77 % and 39.4% respectively. Further analysis shows that the diffraction pattern of the as obtained nanoparticles is different to that in the pattern. The peak was wider for the nanoparticles (FWHM=8.3°) than the MCC (FWHM=2.3°), which mean a greater content of amorphous material in the CNP (Thygesen *et al*., 2005) and/or a refining of the structure. This can be associated with a greater degree of breakup of the cellulose chains, leaving a larger amount of C4 free (Liitiä *et al*., 2003). Thygesen *et al*., (2005) mentioned that peaks (110') in 2θ= 16.5°; (110) in 2θ = 15°; and (200) 2θ = 22.7° are associated with

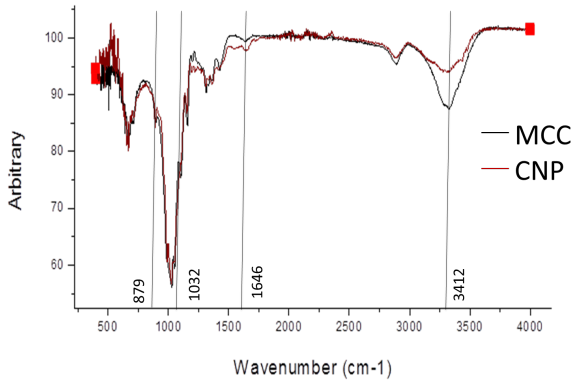

Fig. 2. FTIR spectra of microcrystalline cellulose (MCC) and cellulose nanoparticles from agave waste (CNP).

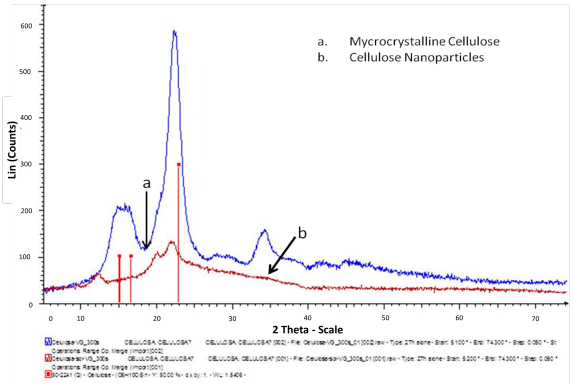

Fig. 3. XRD of microcrystalline cellulose (a) and cellulose nanoparticles (b).

the crystalline diameter on a perpendicular direction to the axis of the cellulose fibers. It can be seen that the reference peak coincides with nanoparticles peak, which indicates that the nanoparticles are mainly constituted by cellulose. This achievement could be important due to having crystalline and amorphous regions and free C4s; these could cause more reactivity with other compounds to accomplish the nanoparticle functionalization (Bolio-Lopez *et al*., 2013). Also, Figure 3 shows a diffractogram of MCC (blue line) and according to the peak identification it is a sample of native cellulose, while the red line shows that the CNP could be either cellulose Iα or cellulose II but it fits better to the peaks of cellulose II, meaning that the purified cellulose had a change in the crystallinity orientation of the unitary cell going from monoclinic to triclinic structure (Colodette, 1989).

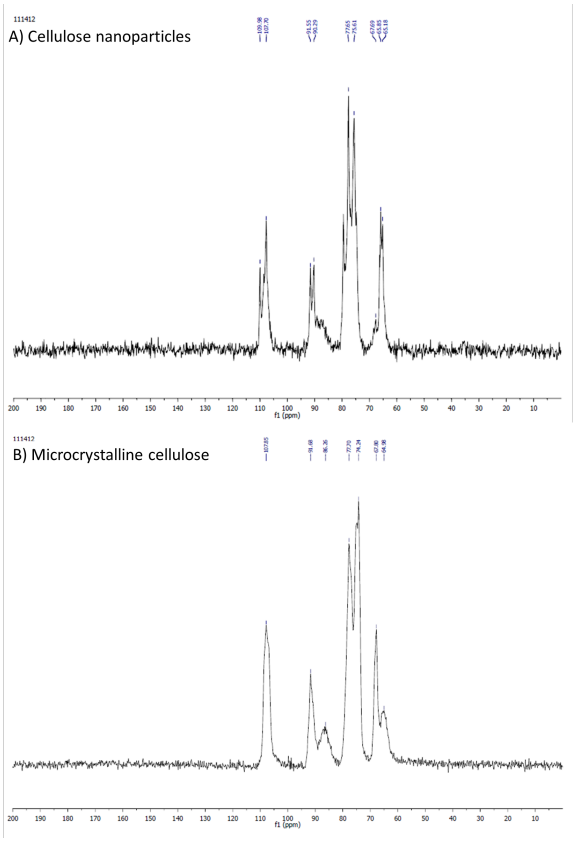

Fig. 4. ssNMR of cellulose nanoparticles (A) and microcrystalline cellulose (B).

In case of ssNMR spectrum of CNP several signals were observed as sharp peaks at 65, 67, 75, 77, 90, 91, 107 and 109 ppm (Figure 4a), that is consistent with the ones reported by Ali *et al.* (1996) for microcrystalline cellulose; who assigned the signals as 60-68 ppm for C6, 70-78 ppm for C2, 3, 5; 80-90 ppm C4 and 100-110 ppm for C1 on the pyranose ring, which are shown in ssNMR spectrum of MCC that was used as reference (Figure 4b). Also, in another report, these peaks were assigned to crystallite interiors of the cellulose (VanderHart and Atalla, 1984). On the other hand, in Figure 4a, there could be observed the peak at 89 ppm decreased, which, according to Horii *et al.*, (1984) is consistent with amorphous cellulose. The differences between the intensities of the peaks for C2 and C6 of ssNMR spectra of CNP and MCC could be due to a conformational change in the "chair" structure of glucose, because the in native state or MCC, the cellulose is type I, while for the CNP the cellulose is type II, due to the alkaline treatment used in their obtention. The ssNMR results compliment the XRD analysis and confirm the crystalline nature of the cellulose nanoparticles.

3.3 Molecular structure of nanoparticles by HRTEM

The high resolution transmission electron microscopy (HRTEM) allows observation of the molecular structure of the CNP can be observed and the interplanar arrangements of the carbon chains and amorphous zones are shown (Figure 5a). These structures are similar to the molecular model proposed by Baird *et al.*, (2008) for Cellulose II. For the structural analysis, one section of the image was cropped and a Fast Fourier Transformation (FFT) obtained. The diffraction pattern was also recorded during the microscope image capture. Both images were compared and the planar lights had to be identified; thus the interplanar distances of 1.2 Å were measured between chains and the angles of the cellulose chains. These results are similar to those reported by Nishiyama *et al.*, (2003) from which a comparison is shown in Table 1. The cellulose nanoparticles could present a triclinic crystalline structure similar to the one proposed by Nishiyama *et al.*, (2003) for fibers from the cell wall of *Glaucocystis nostochinearum* (aquatic algae). This corroborates that the crystalline structure of the nanoparticles correspond to the crystalline structure of cellulose II. Figure 5b shows the electronic diffraction pattern obtained from the nanoparticle zone showed in Figure 5a. Figure 5e shows a model of the angles obtained from the FFT and the diffraction pattern for the cellulose chains. This corresponds to a triclinic structure Figure 5f. The masking on the FFT allows a clearer visualization of the angles that shape the crystalline part of the nanoparticles (Figure 5e). The typical angles of a triclinic structure must be different to 90°and the other angles must differ according to $\alpha \neq \beta \neq \gamma \neq 90$ (Figure 5f). Using this method, only two angles of the crystalline structure can be determined (β and γ). Values shown in Table 1 showed that β=103.4° y γ=76.82° (Figure 5e), confirming that both angles are different to 90°. The α angle cannot be calculated with the TEM image alone because the depth and the B distances cannot be measured (Figure 5f). Figure 5c show a nanoparticle image and amorphous and crystalline zones, from which the FFT was obtained (Figure 5d) to get a similar pattern to the one observed in Figure 5b. This was used to estimate the interplanar distances ("a" and "c") and to draw the rhomboidal structure of one of the faces from the triclinic crystalline arrangement in the nanoparticles cellulose chains. These measurements were similar to the ones reported by Nishiyama *et al.*, (2003).

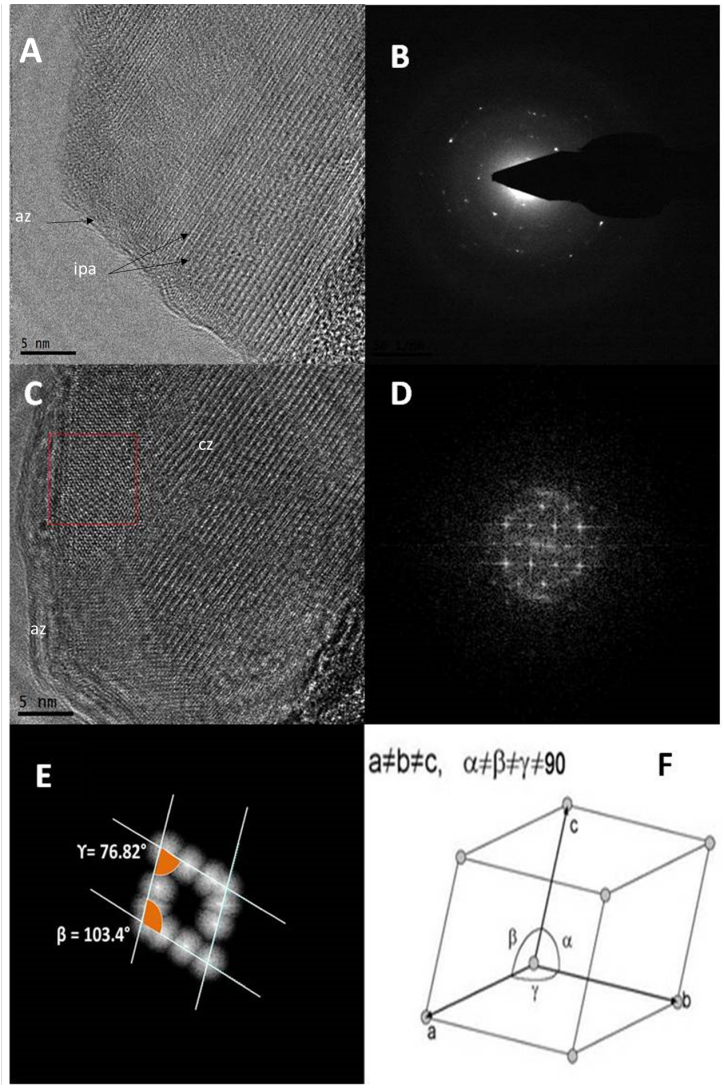

Fig. 5. A) TEM image of a cellulose nanoparticle (CNP), B) Diffraction pattern from the CNP, C) CNP showing the amorphous zones and the crystalline zone, D) Fast Fourier transformation from the TEM image, E) Masking and measurement of the angles from the diffraction pattern, F) Triclinic structure of CNP. az: amorphous zone and ipa: the interplanar arrangements, cz: crystalline zone.

Table 1. Nanoparticle crystal parameters of cellulose nanoparticles (CNP) obtained from agave waste and algae obtained by Nishiyama *et al*. (2003)

Crystal parameters	CNP agave	CNP algae
Crystalline shape	Triclinic	Triclinic
a (Å)	6.31	6.717
c (Å)	10.1	10.400
β(°)	103.4	114.80
γ(°)	76.82	80.37

Conclusion

A facile methodology was established to produce quasi-spherical and polyhedral cellulose nanoparticles from agave *atrovirens* waste. Using SEM imaging, the nanoparticles were observed to have an average size of 97± 30 nm in a range between 31-198 nm with a normal particle size distribution. Cellulose nanoparticles possessed crystalline zones with a triclinic structure elucidated from HRTEM images and XRD diffractograms. The ssNMR and FITR results complimented the structural analysis and confirm

the crystalline nature of the cellulose nanoparticles. These results, suggest that these zones correspond to type II cellulose. Due to the crystallinity index of the cellulose nanoparticles (39.4 %) and the various amorphous zones, this CNP can be easily functionalized and could be used as polymer reinforcers.

Acknowledgements

Claudia Ericka Ponce Reyes wishes to thank CONACyT for the scholarship provided for her studies and international stay. This research was funded through projects 20110627 and 20121001, 20130333 and 20140387 at the Instituto Politécnico Nacional (SIP-IPN Mexico) and133102 of CONACyT

Nomenclature

CNP	cellulose nanoparticles
I_{AM}	intensity of the amorphous zone
I_{200}	highest peak on the diffractogram
FFT	fast Fourier transformation
FTIR	Fourier transformation infrared
HRTEM	high resolution transmission electron microscopy
MCC	microcrystalline cellulose
RCF	revolutions of centrifuge force
SEM	scanning electron microscopy
ssNMR	solid state nuclear magnetic resonance
xCR	crystallinity index
XRD	X-ray diffraction

References

Ali, M; Apperley, D; Eley, C; Emsley, A; Harris, R. (1996). A solid-state NMR study of cellulose degradation. *Cellulose 3*, 77-90.

Ansari, A; Naziruddin, M; Alhosan, M; Aldwayyan, A. (2010). Nanostructured materials: classification, properties, fabrication, characterization and their applications in biomedical sciences. *Nanoparticles: properties, classification, characterization and fabrication*. Nova. New York. 1:1-78.

Askeland, D. (1987). *La Ciencia e Ingeniería de los Materiales*. Grupo Editorial Iberoamérica. México, D.F.

Baker, R; Coburn, S; Liu, C; Tetteh, J. (2005). Pyrolysis of saccharide tobacco ingredients: a TGA-FTIR investigation. *Journal of Analytical and Applied Polymers 74*, 171-180.

Baird, M.S; Hamlin, J.D; O?sullivan, A; Whiting, A. (2008). An insight into the mechanism of the cellulose dyeing process: Molecular modeling and simulations of cellulose and its interactions with water, urea, aromatic azo-dyes and aryl ammonium compounds. Dyes and Pigments.

Blackwell, J. Kolpak, F.J, Gadner, K.H. (1987). Structures of Native and Regenerated Celluloses, The Structures of Cellulose. *Characterization of the solid States*. Rajai H. Atalla Editor, American Society. Washington D.C.

Bolio-Lopez, G.I., Valadez-Gonzalez, A., Veleva, L., Andreeva, A. (2011). Whiskers de celulosa a partir de residuos agroindustriales de banano: obtención y caracterización. *Revista Mexicana de Ingeniería Química 10*, 291-299.

Bolio-Lopez, G.I., Veleva, L., Valadez-Gonzalez, A. and Quintana-Owen, P. (2013). Weathering and biodegradation of polylactic acid composite reinforced with cellulose whiskers. *Revista Mexicana de Ingeniería Química 12*, 143-153.

Burr, I.W. (1942). Cumulative frequency functions. *Annals of Mathematical Statistics 13*, 215-232.

Colodette, J.L. (1989). *Química da Madeira Vicosa*. *UFV 50*, 201-338.

Coronel, E. O. (1994). *Fundamentos de las propiedades físicas y mecánicas de las maderas*. Primera Parte. Facultad de Ciencias Forestales. Universidad Nacional Santiago del Estero. Argentina. p.13-28.

Cruz-Estrada, R.H., Fuentes-Carrillo P., Martínez-Domínguez O., Canché-Escamilla G. and García-Gómez C. (2006). Obtención de materiales compuestos a base de desechos vegetales y polietileno de alta densidad. *Revista Mexicana de Ingeniería Química 5*, 29-34.

Elazzouzi-Hafraoui, S. Nishiyama, Y. Putaux, J.L. Heux, L. Dubreuil, F. And Rochas, C. (2008). The Shape and Size Distribution of Crystalline Nanoparticles Prepared by Acid Hydrolysis of Native Cellulose. *Biomacromolecules 9*, 57-65.

García-Mendoza, A. (2002). Distribution of the genus Agave (*Agavaceae*) and its endemic species in Mexico. *Cactus and Succulent Journal 74*, 177-187.

García, R . M; Flores, N; Martínez, H. E; Rutiaga, J. G. Identificación y caracterización de nanocristales de Celulosa obtenidos mediante emulsión inversa y Ultrasonicación térmica. *X National Congress of Microscopy*. Morelia, Mich. 2010.

Gil Vega,K; González Chavira, M; Martínez de la Vega, O; Simpson, J; Vandemark, G. (2001). Analysis of genetic diversity in Agave tequilana var. Azul using RAPD markers. *Euphytica 119*, 335-341.

Gradwell, S. E., Renneckar, S., Esker, A. R., Heinze, T., Gatenholm, P., Vaca-Garcia, C. (2004). Surface modification of cellulose fibers: towards wood composites by biomimetics. *Comptes Rendus Biologies 327*, 945-953.

Gumeta-Chávez, C; Chanona-Pérez, J.J; Mendoza-Pérez, J.A; Terrés-Rojas, E; Garibay-Febles, V; Gutiérrez-López, G.F. (2011). Shrinkage and Deformation of Agave atrovirens Karw Tissue during Convective Drying: Influence of Structural Arrangements. *Drying Technology 29*, 612- 623.

Hepworth, D. (2000). The Mechanical Properties of a Composite Manufactured from Non Fibrous Vegetable Tissue y PVA. *Composites. Part A. 31*, 283-285.

Horii, E, Hirai, A. and Kitamaru, R. (1984). CPMAS carbon-13 NMR study of spin relaxation phenomena of cellulose containing crystalline and noncrystalline components. *J. Carbohydr. Chemi. 3*, 641-662.

Hubbe, M; Rojas, O; Lucia, L; Sain, M. (2008). Cellulosic Nanocomposites: a review. *BioResources 3*, 929-980.

Inpanya, P; Faikrua, A; Ounaroon, A; Sittichokechaiwut, A; Viyoch, J. (2012). Effects of the blended fibroin/aloe gel film on wound healing in streptozotocin-induced diabetic rats. *Biomedical Matter 7*, 1-14.

Kallioranta, S. (2012) Who is in control in the packaging industry? Paper 360º. *TAPPI 7*, 14-16.

Liitiä, T; Maunu, S.L; Hortling, B; Tamminen, T; Pekkala, O; Varhimo, A. (2003). Cellulose crystallinity and ordering of hemicelluloses in pine and birch pulps as revealed by solid-state NMR spectroscopic methods. *Cellulose 10*, 307-316.

Macia, M. (2006). The fiber plants. *Revista Botánica Económica de los Andes Centrales*, 370-384.

Narvaez-Zapata, J; Sánchez-Teyer, l. (2009). Agave as a raw material: Recent technologies and applications. *Recent Patents on Biotechnology 3*, 185-191.

Nishiyama, Y; Sugiyama, J; Chanzy, H; Langan, P. (2003). Crystal Structure and Hydrogen Bonding System in Cellulose I? from Synchrotron X-ray and Neutron Fiber Diffraction. *JACS articles*, published in Web.

Nyström, G; Mihranyan,A; Razaq, A; Lindström, T; Nyholm, T; Strømme, M. (2010). A Nanocellulose Polypyrrole Composite Based on Microfibrillated Cellulose from Wood. *Journal of Physcal Chemistry 114*, 4178-4182.

Qing, Y; Sabo, R; Wu, Y; Cai, Z. (2012). High-Performance cellulose nanofibril composite films. *BioResouces 7*, 3064-3075.

Ragauskas, A. J., Williams, C. K., Davison, B. H., Britovsek, G., Cairney, J., Eckert, C. A. (2006).The path forward for biofuels and biomaterials. *Science 311*, 484-489.

Samir, M. A. S. A; Alloin, F; Dufresne, A. (2005). Review of recent research into cellulosic whiskers, their properties and their application in nanocomposite field. *Biomacromolecules 6*, 612-626.

Siqueira, G; Bras J; Dufresne, A. (2009). Cellulose Whiskers versus Microfibrils: Influence of the Nature of the Nanoparticle and its Surface Functionalization on the Thermal and Mechanical Properties of Nanocomposites. *Biomacromolecules 10*, 425-432.

Tang, E.O., Chow, D.C.: US20060222719 (2006).

Thygesen, A; Oddershede, J; Liholt, H; Thomsen, A.B; Sta, K. (2005). On the determination of crystallinity and cellulose content in plant fibres. *Cellulose 12*, 563-576.

VanderHart, D. L.; Atalla, R. H. (1984). Studies of microstructure in native celluloses using solidstate 13C NMR. *Macromolecules 17*, 1465-1472.

Zhang, J., Elder, T., Pu, Y., Ragasukas, A. (2007). Facile synthesis of spherical cellulose nanoparticles. *Carbohydrate Polymers 69*, 607-611.